Materials & Design 215 (2022) 110421

Contents lists available at ScienceDirect

Materials & Design

journal homepage: www.elsevier.com/locate/matdes

Structural and mechanical evolution of the multiphase asphalt rubber during aging based on micromechanical back-calculation and experimental methods

Danning Li [a], Zhen Leng [a,*], Haopeng Wang [b], Ruiqi Chen [a], Frohmut Wellner [c]

[a] Department of Civil and Environmental Engineering Department, The Hong Kong Polytechnic University, Kowloon, Hong Kong
[b] Nottingham Transportation Engineering Centre, University of Nottingham, Nottingham, UK
[c] Institute of Urban and Pavement Engineering, Technische Universität Dresden, Dresden, Germany

HIGHLIGHTS

- Aging caused structural change in asphalt rubber with deteriorated rubber swelling.
- The micromechanical back-calculation correlated well with experimental results.
- The degradation of natural rubber increased the stiffness of crumb rubber.
- The swelling rubber yielded less mechanical contribution after aging.

GRAPHICAL ABSTRACT

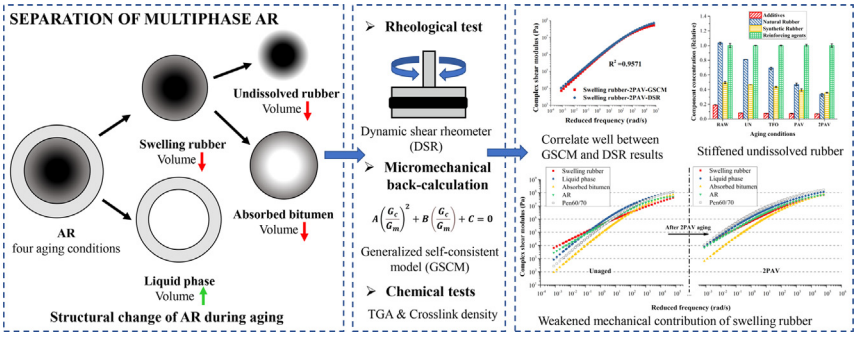

ARTICLE INFO

Article history:
Received 10 August 2021
Revised 20 January 2022
Accepted 20 January 2022
Available online 25 January 2022

Keywords:
Asphalt rubber
Bitumen aging
Micromechanics
Back-calculation
Chemical characterization

ABSTRACT

Asphalt rubber (AR) is a sustainable paving material composed of bitumen and crumb rubber modifier (CRM) recycled from waste tires. The interaction between bitumen and CRM re-distributes the bitumen fractions and creates a multiphase internal structure of AR. Although the superior aging resistance of AR has been acknowledged, the aging mechanism of AR remains unclear due to the limited understanding on the behaviors of different phases of AR during aging. This study aims to investigate the structural and mechanical evolution of AR binder during aging through micromechanical back-calculation and experimental tests. A series of separation methods were used to disintegrate the multiphase system of AR at four aging conditions. The mechanical properties of different phases obtained from frequency sweep tests and their volumetric fractions were used as the input for the micromechanical back-calculation, which yielded accurate prediction for the complex modulus of swelling rubber but failed for that of undissolved rubber, so further chemical characterization was conducted to estimate its mechanical evolution. The results indicated that the aging of AR is a process in which internal multiphase structures changed simultaneously with mechanical properties. All subphases became stiffer but their influences on the overall mechanical property of AR variated after aging.

1. Introduction

Recycling waste tires into crumb rubber modifier (CRM) for bitumen modification has become a prevailing way to improve

* Corresponding author.
E-mail address: zhen.leng@polyu.edu.hk (Z. Leng).

https://doi.org/10.1016/j.matdes.2022.110421
0264-1275/

the durability and environmental benefits of asphalt paving material. According to different preparation methods, several types of rubberized asphalt materials can be produced while asphalt rubber (AR) is the one that consumes CRM the most [1,2]. AR binder is produced by a high-shear mixing of bitumen and at least 15% of CRM by weight of the total binder at 175–200 °C for 30–90 min [3]. When used as a paving material, AR provides enhanced rutting and fatigue resistance as well as numerous environmental and economic benefits. Therefore, it has gained fast-growing interest in many countries during the past decades [4–6]. Although some drawbacks of AR exist, such as poor workability and storage stability, researches have shown that these concerns can be effectively reduced by warm mix asphalt (WMA) technology, surface activation, nanotechnology, etc [7–10]. With the increasing application of AR pavement around the world, one inevitable problem emerges when its service life expires, which is the unclear recyclability of the reclaimed AR pavement (RARP) due to the insufficient understanding of aging mechanisms of AR.

Compared with raw bitumen and common polymer modified bitumen, the more intricate aging and recyclability mechanisms of AR originate from the complex composition of CRM and its interaction with bitumen. The main components of CRM include natural rubber (NR), synthetic rubber (SR), reinforcing agents (carbon black, amorphous silica), and other additives like processing oil, surfactants, and antioxidants [11]. Among various components of CRM, the rubber polymers, carbon black, and anti-oxidants have been found to mitigate the oxidation of bitumen during aging and improve the aging resistance [12–14]. Despite this, the swelling and dissolution of CRM in bitumen is the main reason that differs the aging behaviors of AR from other bitumen. When CRM interacts with bitumen at high temperatures, the light fractions of bitumen are absorbed into the rubber polymer network, amplifying its volume by 3–5 times [15]. On the other hand, the dissolution of CRM can be comprehended as the physical size reduction of CRM and the chemical degradation of rubber polymers during preparation and aging process [11,16]. The combination of these two behaviors leads to the partially swelling and partially dissolved state of rubber in bitumen, forming the multiphase structure of AR. The multiphase system of AR can be divided into liquid phase (non-absorbed bitumen) and swelling rubber, while the swelling rubber can be further divided into the absorbed bitumen and the undissolved rubber.

The swelling degree and dissolution level of rubber determine the composition and the microstructure of AR system. While considerable work has been done to investigate the rubber swelling mechanisms in bitumen [17–19], how the swelling degree of rubber changes during aging due to the increasing amount of asphaltenes and the rubber degradation remain unclear. Although a recent study has demonstrated that the rubber absorption behaviors can maintain a relatively stable mechanical property of swelling rubber throughout the aging process [20], little is known about the structural and mechanical evolution of different phases and their influence on the overall property of AR during aging. However, it is challenging to directly measure the varying mechanical condition of rubber in AR during aging due to the difficulty of sample preparation and limitation of testing method. To address this challenge, the analytical micromechanical model can be considered as a potential tool.

Continuum mechanics-based micromechanical models have increasingly been used to predict the mechanical properties of bituminous materials for their merits of efficiency and effectiveness [21]. Complex shear modulus is one of the most important mechanical parameters for bituminous materials. So far, several attempts have been made to use micromechanical models to predict the complex shear modulus of rubberized bitumen with known properties of the constituents. Medina and Underwood [16] used Hashin and Christensen Models to predict the complex shear modulus of activated crumb rubber bitumen by using rheological testing and electron microscopy to obtain the input parameters. In a comparative study, Wang et al. [22] suggested that the generalized self-consistent model (GSCM) owned superior accuracy than several other analytical micromechanical models in predicting the complex modulus of AR binder with a high concentration of CRM. However, very limited study has tried to use it in a reverse way to calculate the property of individual constituent within the composite. Only one study conducted by Jamrah et al. [23] combined experimental programs and finite element based micromechanical model to back-calculate the modulus of swollen rubber and relate it to the macroscale material behavior.

To further understand the aging and recycling mechanisms of AR, this study aims to investigate the structural and mechanical evolution rules of AR during aging. A combined method of micromechanical modeling and experimental tests were applied to characterize the properties of each phase in AR. The flowchart of this study is shown in Fig. 1. AR binders at four different aging conditions were separated into multiple sub-phases and their mass and volume fractions were measured. Rheological and chemical tests were conducted on different phases to characterize their mechanical property or chemical composition. The GSCM was selected for the modeling of AR binder with the input parameters obtained from experimental tests and the generalized reduced gradient (GRG) nonlinear solving algorithm was used for the back-calculation. The findings of this study are expected to shed light on the fundamental aging mechanism of AR and provide reference for developing effective recycling approaches.

2. Experimental program

2.1. Sample preparation and aging procedure

A bitumen commonly used in Hong Kong with a penetration grade of 60/70 (Pen60/70) was used as the raw binder, whose basic properties are shown in Table 1. CRMs ambiently grinded from end-of-life truck tires with a particle size between 0.3 and 0.5 mm were collected. A typical wet-process high viscosity AR binder was produced by using a high shear mixer to blend 20% CRM (by mass of raw bitumen) into raw bitumen at 180 °C and 4000 rpm for 60 min. Using such preparation procedure can ensure the sufficient swelling of rubber, forming the multiphase structure of AR. Meanwhile, the AR prepared by this procedure has been proved to own superior rheological performance and aging resistance [18,20].

A series of laboratory aging procedures were conducted to age the AR binder. To simulate short-term aging, the standard rolling thin film oven (RTFO) test was replaced by a thin film oven (TFO) test as proposed by Wang et al. [12]. 20 g of AR binder was uniformly applied on a plate of 140 mm diameter to form a thin film of 1.25 mm thickness, which was then placed in a 163 °C oven with a horizontally spinning shelf for 2 h. In the TFO method, AR binder can be more evenly aged and easier to remove from a plate than the bottle used in the RTFO test. Meanwhile, standard pressure aging vessel (PAV) test was conducted for simulating the long-term aging, where 50 g TFO-aged AR binder was poured onto a 140 mm-diameter pan to form a film of 3.2 mm thickness. The temperature and pressure of the vessel were set as 100 °C and 2.1 ± 0.1 MPa, respectively. Two aging durations, 20 and 40 h, were applied. To sum up, four aging conditions of AR binders were prepared for testing, including unaged, TFO-aged, 20-hour PAV-aged, and 40-hour PAV-aged, which were labeled as UN, TFO, PAV, and 2PAV, respectively, in this paper.

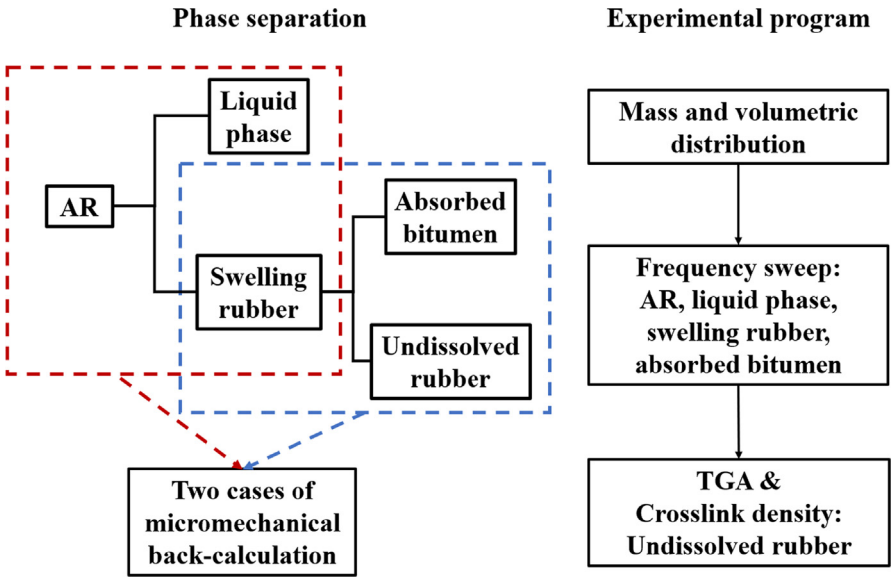

Fig. 1. Flowchart of this study.

Table 1
Basic properties of raw bitumen.

Item		Method	Unit	Result
Penetration at 25 °C		ASTM D5	0.1	63.5
Softening point		ASTM D36	°C	48.2
Ductility at 10 °C		ASTM D113	cm	32
Viscosity at 135 °C		AASHTO T316	mPa·s	446
SARA fraction	Saturates	ASTM D4124	wt%	17.58
	Aromatics			46.85
	Resins			26.20
	Asphaltenes			59.37

2.2. Phase separation of AR binder

The interaction between bitumen and CRM created the multiphase system of AR, which can be separated into liquid phase (non-absorbed bitumen fractions) and swelling rubber, while the swelling rubber is comprised of absorbed bitumen fractions and undissolved rubber. To investigate the role of each component in the mechanical property of AR, a series of phase separation tests were conducted, as illustrated in Fig. 2. Firstly, AR binders at different aging conditions were poured onto a 200-mesh sieve net and stored in an oven of 175 °C for 15 min so that the liquid phase could flow through the sieve holes and leave the swollen rubber on the sieve net. A cap was used to seal the sieve to reduce the contact of binder with air and the whole device was put into a refrigerator immediately after the separation to avoid any further aging. Complete separation of swollen rubber and liquid phase was achieved when no liquid bitumen drip can be observed from the downside of the sieve net. Secondly, the sieve net containing swollen rubber was wrapped up and put into the Soxhlet extractor. Soxhlet extraction is a method of separating soluble substances from insoluble solids by using specific solvents based on the solvent reflux and siphonage, which allows unmonitored and unmanaged operation while efficiently recycling a small amount of solvent. The dichloromethane (DCM) solvent was used in this study because it has a very low boiling point (39.5 °C). The whole Soxhlet extraction device consisted of a Soxhlet extractor, a condenser, a flask, and an oil heating pot. The extraction ended when the DCM solvent condensed in the Soxhlet extractor became transparent and colorless, where the undissolved rubbers were left inside the sieve net and the absorbed bitumen fractions were dissolved in the flask containing DCM solvent. Subsequently, the absorbed bitumen fractions dissolved in the DCM solvent were reclaimed by the evaporation method. Three replicates were prepared for both separation methods, and the mass ratio of each phase was recorded. The errors of mass ratios for different samples were all less than 3%, which indicates high repeatability of the adopted separation methods. It should be noted that in this study the dissolution of CRM includes not only the degraded and desulfurized rubber polymers and other components released into the bitumen matrix, but also the microscale CRM particles possibly shed or split from large CRM particles during preparation and aging that can pass the 200-mesh sieve net (particle size < 0.075 mm). Such definitions have been adopted by many studies concerning the binary system of AR [16,24,25].

2.3. Mass and volume measurements of different phases

After the AR, liquid phase (LP), absorbed bitumen fractions (AB), and undissolved rubber (UR) were obtained, their theoretical maximum specific densities (ρ_{mm}) were measured based on Archimedes' principle. Since it is easy to generate relatively large errors when measuring the density of powder or microparticles, the density of undissolved rubber was not directly measured. Each bituminous sample (except undissolved rubber) was heated and poured into a silica gel mold, and then stirred by a glass stick to expel the air. When the sample was cooled to room temperature, it was removed from the mold and its mass in air (M_{air}) was weighted. Subsequently, the sample was placed in a beaker filled

Fig. 2. Phase separation process of the AR binder.

with water, and then the beaker was placed directly into a vacuum container with a residual pressure of 10 kPa for 30 min to further remove the air from the sample. Finally, the sample was quickly transferred into the water tank of the scale and its mass in water (M_{liq}) was weighted. Three replicates were tested. The ρ_{mm} of different samples can be calculated by Equation 1.

$$\rho_{mm} = M_{air}\rho_w/(M_{air} - M_{liq}) \quad (1)$$

where ρ_w = 0.997 g/cm^3, which is the density of water at 25 °C.

Table 2 summarizes the density and mass ratios of different phases in AR binder at different aging conditions. Obvious changes can be found in the mass distribution of different phases during aging, revealing the complex aging mechanism of AR. The volume fractions of each phase were then calculated and served as input parameters for the micromechanical modeling. The volume fractions of undissolved rubber were calculated by subtracting the total volume of other phases from the volume of AR. More detailed discussion is provided in the results and discussion section.

2.4. Frequency sweep test

An Anton Paar dynamic shear rheometer (DSR) was used to measure the complex shear modulus of AR, liquid phase, swelling rubber, and absorbed bitumen in a large frequency range. Since this study focuses on the effect of aging on the overall rheological property of AR binder, frequency sweep tests were conducted on samples at four aging conditions. By doing so, the master curve of each sample at different aging conditions can be established to the evolution of their mechanical property. The temperature range was 10–60 °C with an interval of 10 °C. Plates of 25 mm and 8 mm diameter were used for tests at 40–60 °C and 10–30 °C, respectively. The strain level of samples was controlled as 0.1% at 16

Table 2
Mass ratio and density results.

Aging Conditions	Mass ratio (%)				Theoretical maximum specific gravity (ρ_{mm} at 25 °C) (g/cm^3)		
	AR	LP	AB	UR	AR	LP	AB
UN	100	25.355	60.404	14.241	1.054	1.051	1.035
TFO	100	23.430	63.100	13.470	1.052	1.052	1.029
PAV	100	30.906	59.080	10.014	1.053	1.050	1.037
2PAV	100	37.689	53.557	8.754	1.052	1.052	1.042

specified frequencies between 0.1 and 100 Hz for each testing temperature to maintain its linear viscoelasticity. The shift factors were calculated by the Williams-Landel-Ferry (WLF) equation as shown below:

$$\log \alpha_T(T) = \frac{-C_1(T - T_{ref})}{C_2 + (T - T_{ref})} \tag{2}$$

where $\alpha_T(T)$ is the shift factors; C_1 and C_2 are coefficients of regression; T is the experimental temperature; and T_{ref} is the reference temperature, which is 25 °C in this study. In addition, a modified Christensen-Anderson-Marasteanu (CAM) model was adopted for fitting the master curves of complex modulus as shown below:

$$G^* = \frac{G_g^*}{[1 + (f_c/f_r)^k]^{\frac{m}{k}}} \tag{3}$$

where G^* represents the complex shear modulus, Pa; G_g^* is the glass complex shear modulus as the frequency approaches infinity, Pa; f_r is the reduced frequency, rad/s; f_c is the crossover frequency, rad/s; and k, and m are fitting coefficients.

$$\delta = 90I - \frac{90I - \delta_p}{\left\{1 + \left[\frac{\log(f_p/f_r)}{R_d}\right]^2\right\}^{\frac{m_d}{2}}} \tag{4}$$

where δ is the phase angle, °; δ_p is the value of the inflection point of the phase angle master curve, °; f_p is the location parameter at which δ_p occurs, rad/s; R_d and m_d are fitting coefficients; and $I = 0$ if $f_r > f_p$, $I = 1$ if $f_r \le f_p$.

2.5. Thermal gravimetric analysis (TGA) test

As a useful tool for determining the composition of tire rubber, TGA tests were conducted on raw CRM and undissolved rubber residues at four aging conditions as references for their mechanical evolution of property during aging. A Rigaku instrument (Thermos Plus Evo 8121) with nitrogen gas at a flow rate of 250 ml/min was used. About 5 mg of sample was used for each test, which was heated from ambient temperature to 700 °C with a heating rate of 10 °C/min. The weight losses of a sample at different temperature ranges were recorded to represent the proportion of corresponding components in the tire rubber.

2.6. Crosslink density measurement

The crosslink density of tire rubber, which can be regarded as an indicator of the mechanical property, was determined by the swelling solvent method and calculated based on the Flory-Rehner theory [11]. Approximately 1.2 g of undissolved rubber residues at four aging conditions were wrapped by the 200-mesh sieve net and soaked into toluene solvent for 72 h. The local volume fraction of rubber in a swollen state (Q) was calculated by:

$$\phi_r = V_0/(V_0 + V_1) \tag{5}$$

where V_0 is the volume of the dry rubber and V_1 is the volume of the toluene absorbed by rubber, cm^3. Subsequently, the crosslink density was calculated by:

$$v_x = -\frac{\ln(1 - \phi_r) + \phi_r + \chi\phi_r^2}{\varphi_b(\phi_r^{\frac{1}{3}} - \frac{1}{2}\phi_r)} \tag{6}$$

where v_x is the crosslink density of rubber, mol/cm^3; χ is the interaction parameter between rubber and toluene, which is taken as 0.4 according to Yao et. al [26]; and φ_b is the molar volume of the toluene solvent, which is 106.29 mol/cm^3.

3. Micromechanical modelling

3.1. Homogenization theory

When applying continuum mechanics-based micromechanical models to describe the effective mechanical properties of heterogeneous composites like bituminous materials, one important strategy is to apply the homogenization theory to the composite, which can be understood as a homogeneous representative volume element (RVE) filled by multiple sub-phases [27]. In view of this concept, constituents with the same mechanical properties are usually regarded as one phase. When subjected to a macroscopic load, the stress and strain of each phase can be related to the overall modulus of the composite [28]. Therefore, a reasonable division of the composite and accurate determinations of the input parameters, namely the volumetric fractions and mechanical properties of various phases, significantly influence the accuracy of prediction.

3.2. Generalized self-consistent model (GSCM)

In this study, the three-phase GSCM established by Christensen and Lo [29] was utilized to describe the multiphase system of AR. The GSCM describes a composite where a spherical inclusion embedded in a spherical matrix possesses the same effective mechanical properties as the surrounding equivalent homogeneous media. The formulation for the GSCM is given in a quadratic form as follows:

$$A\left(\frac{G_c}{G_m}\right)^2 + B\left(\frac{G_c}{G_m}\right) + C = 0 \tag{7}$$

where G_c and G_m are the moduli of the composite and the matrix, respectively; A, B, and C are functions comprising the mechanical properties and volume fraction of inclusions and matrix, including modulus, Poisson's ratio, and volumetric concentration. The lengthy equations of A, B, and C are listed in Appendix A.

3.3. Back-calculation of inclusion's modulus using GSCM and GRG algorithm

As aforementioned, most studies in the field of bituminous materials utilized various micromechanical models to predict the overall mechanical property of the composite or mixture, but little effort has been taken to reversely calculate the properties of an individual constituent when the properties of the composite and other constituents are known. Since currently there is no attested experimental method to evaluate the complex modulus of swelling rubber and undissolved rubber, a back-calculation method based on micromechanical modeling was designed. The idea was to back-calculate the modulus of inclusion in GSCM with known moduli and volume fractions of composite and matrix by the GRG nonlinear solving method, which is an efficient algorithm for the finding locally optimal solution for nonlinear problems [30]. The nonlinear program is in the following form:

$$Minimize\ f(X) \tag{8}$$

$$subject\ to\ g_i(X) = 0, i = 1, \cdots, m \tag{9}$$

$$l_i \le X \le u_i, i = 1, \cdots, n \tag{10}$$

where $f(X)$ is the function to be solved; X is a vector with n variables; $g_i(X)$ are the nonlinear constraints; and l_i, andu_i are given lower and upper bounds. A sequence step method was used where only one inclusion was considered in each step [21]. Firstly, the complex shear modulus of swelling rubber was back-calculated

when treating AR as the composite and liquid phase as the matrix. Furthermore, the swelling rubber and absorbed bitumen were regarded as the composite and matrix to back-calculate the modulus of undissolved rubber as inclusion. The volume fraction inputs were derived from the phase separation test while the modulus inputs were obtained from the master curves built based on frequency sweep test results. The complex shear modulus of swelling rubber calculated from GSCM and those measured by DSR were mutually validated. As for the undissolved rubber residues which cannot be tested by DSR, further chemical characterizations were conducted to estimate the evolution of its mechanical property during aging.

4. Results and discussion

4.1. Preliminary tests

In this study, DCM has been used as the solvent for the extraction of absorbed bitumen. Thus, worries existed if this solvent would influence the properties of the bitumen and CRM particles, which may impair the persuasiveness of this study. To ease such worries, a series of preliminary tests were conducted to evaluate: 1) the mass loss of CRM after soaking in DCM for 24 h; 2) the difference in mechanical properties of bitumen after once dissolved in DCM solvent; and 3) the chemical composition of CRM before and after soaking in DCM solvent for 24 h. Three replicates were prepared and tested for each task. Since they are not the main topics of this study, the process of each preliminary test is not presented in details in this paper.

The results indicated that the mass of CRM only decreased 0.8% after soaking CRM in DCM for 24 h, which may mainly come from the floating-away of some micro-sized CRM from the macroparticles. It indicated that the use of DCM solvent led to insignificant effect on the measurement of mass proportion for the undissolved rubber. Furthermore, the master curves of complex shear modulus and phase angle of raw Pen60/70 and Pen60/70 reclaimed from DCM solvent were compared in Fig. 3, where the two curves are basically overlapped with a minor average error of 3.55%. Thus, the influence of DCM dissolution on the mechanical property of bitumen can be neglected. Finally, the TGA results showed that the ratios of NR, SR, and reinforcing agents in CRM slightly changed from 37.64%, 18.27%, and 38.08% to 38.08%, 18.05%, and 36.79%, respectively, after CRM was soaked in DCM for 24 h. Therefore, it is believed that the DCM solvent did not alter the chemical composition of CRM either. In short, the preliminary tests proved the applicability of the phase separation methods used in this study.

4.2. Volumetric variations of different phases during aging

Based on the mass fractions and density results, the volumetric variations of different phases during aging were calculated and plotted in Fig. 4. At unaged condition, it can be seen that the swelling rubber (absorbed bitumen and undissolved rubber) took up almost 75% of the volume in AR, which reflected the volume expansion of CRM after absorbing the bitumen light fractions during preparation. Meanwhile, the volume fraction of undissolved rubber at unaged condition indicated that about one-third of CRM were dissolved or split into particles smaller than 0.075 mm during the preparation. The proportion of liquid phase slightly decreased after TFO aging conditions due to the further absorption of rubber under high temperature. During the long-term aging, the phase variation became more obvious with a clear increasing trend for the volume fraction of liquid phase and the corresponding decreased volume fractions of absorbed bitumen and undissolved rubber. Representing an internal structural change, the volumetric variations in AR binder can be attributed to two aspects: 1) rubber dissolved during aging so fewer bitumen fractions can be absorbed and stored; 2) the molecular weight of absorbed bitumen fractions increased during aging due to the oxidation and the transformation from aromatics to asphaltenes, so the rubber lost its control on part of the heavier fractions and expelled them into the liquid phase [20].

4.3. Back-calculation of moduli of swelling rubber and undissolved rubber

As a two-step back-calculation method was used, the complex shear modulus of the swelling rubber was back-calculated first and validated with that measured from DSR. It should be noted that this is considered as a mutual validation because there are two concerns when using DSR to measure the complex shear modulus of swelling rubber: 1) the inadequate flowability of swelling rubber could lead to the difficulty of DSR sample preparation including possible internal voids, uneven surfaces, and irregular shapes (see the swelling rubber in Fig. 2); and 2) the swelling rubber particles touching the measuring plates of DSR might cause certain experimental errors. To quantify the discrepancy between the results from two resources, the goodness-of-fit statistical tests were conducted using following equations [31]:

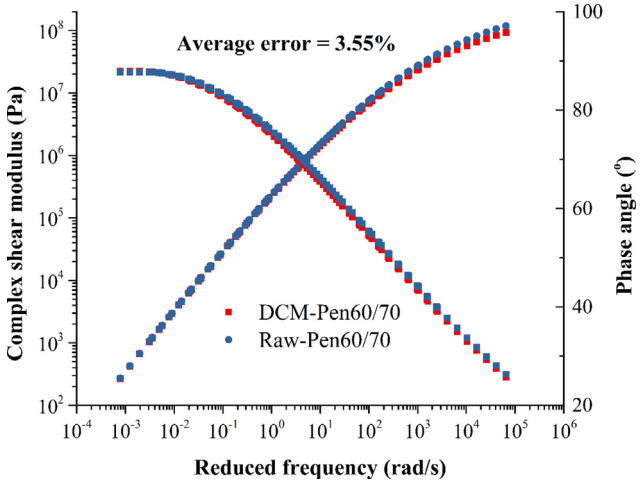

Fig. 3. Comparison of Pen60/70 before and after reclaimed from DCM solvent.

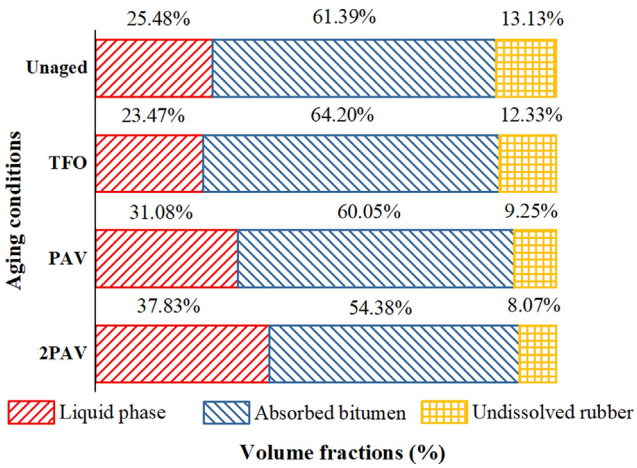

Fig. 4. Volumetric variation of different phases in AR during aging.

$$S_e = \sqrt{\frac{\sum_{i=1}^{n}(G_{Bi}^{*} - G_{Di}^{*})^2}{n-k}} \tag{11}$$

$$S_y = \sqrt{\frac{\sum_{i=1}^{n}(G_{Di}^{*} - \bar{G}_{D}^{*})^2}{n}} \tag{12}$$

$$R^2 = 1 - \frac{n-k}{n-1}\left(\frac{S_e}{S_y}\right)^2 \tag{13}$$

where S_e is the standard error; S_y is the standard deviation; R^2 is the coefficient of determination;n is the number of data points; k is the number of independent variables in the GSCM model; G_{Bi}^{*} is the complex shear modulus back-calculated from GSCM model; and G_{Di}^{*} is the complex shear modulus measured by DSR, whose average value is $\bar{G}_{D}^{*}$. Therefore, the complex shear moduli of swelling rubber from GSCM back-calculation and DSR measurement at four aging conditions as well as their coefficients of determination and relative errors (S_e/S_y) were plotted in Fig. 5. Comparing the two master curves, both GSCM back-calculation and DSR measurement presented the frequency-dependent property of the swelling rubber. The absorption of bitumen light fractions transforms the property of CRM from elastic to viscoelastic, where the complex modulus increased with the increasing frequency [17]. An overall accurate correlation can be found between the two results from different methods. Among four aging conditions, the PAV aged swelling rubber showed the highest coefficient of determination ($R^2 = 0.9983$) and lowest relative error (S_e/S_y = 0.0419). The largest discrepancy appeared at the unaged condition, where the coefficient of determination was 0.8662. However, given the order of magnitude of the unit of complex shear modulus, this relative error can be considered as acceptable. It can therefore be suggested that both GSCM back-calculation and DSR measurement can be used to assess the complex shear modulus of swelling rubber.

In step two, the back-calculation of the undissolved rubber was attempted. Contrary to expectations, the back-calculation failed in this case where the GRG solving method could not converge to a solution for the modulus of undissolved rubber for most of the frequency regions. Assuming the inputs of swelling rubber and absorbed bitumen from DSR are reliable, the reason why the back-calculation aborted could be deduced to the volumetric input parameters. In GSCM, one critical assumption is that the inclusion and matrix have no overlapping area [29]. However, the absorptive behavior of rubber causes strong overlapping volumes between the absorbed bitumen and rubber itself. Fig. 6 offers a possible expla-

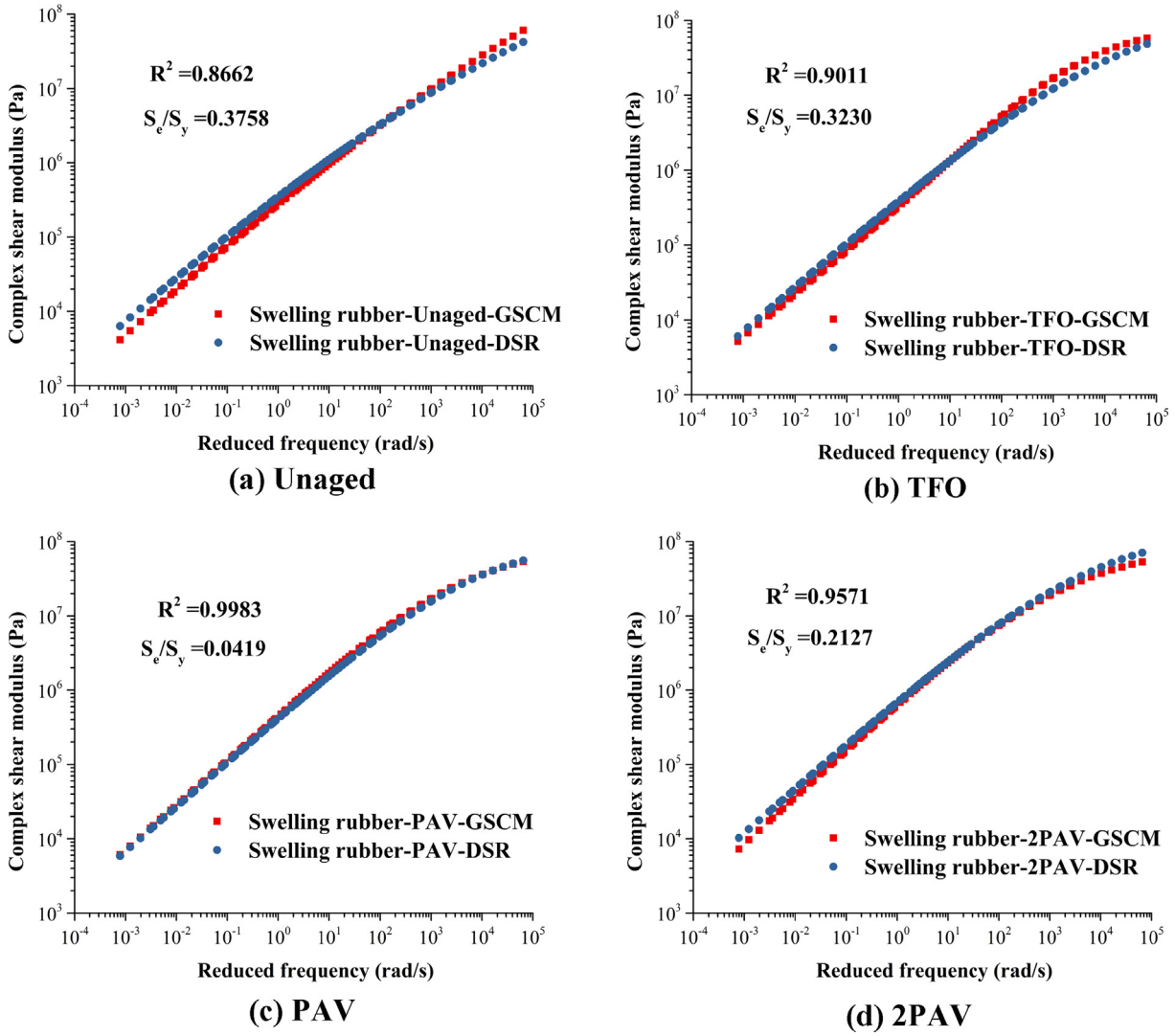

Fig. 5. Complex shear modulus master curves of swelling rubber from GSCM back-calculation and DSR measurement.

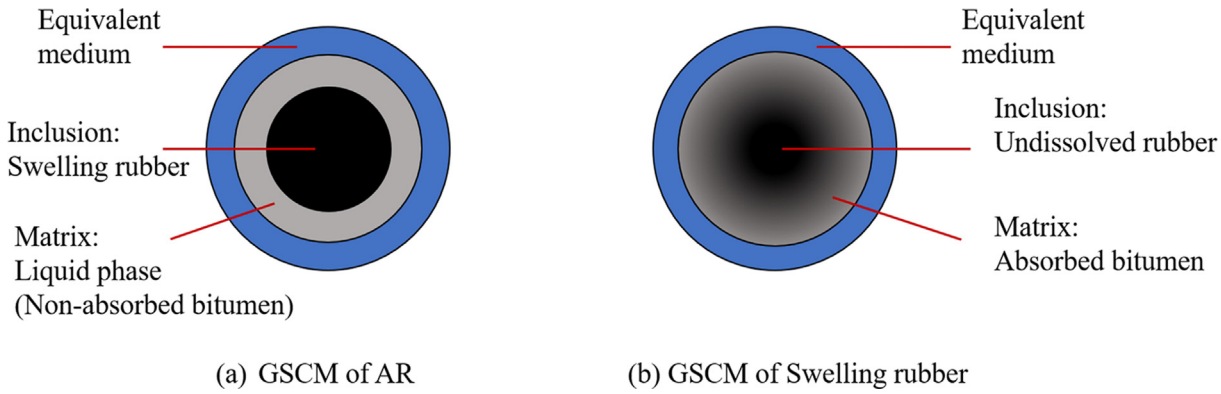

Fig. 6. Schematics of the different GSCMs for AR and swelling rubber.

nation for the difference between the GSCM of AR and swelling rubber. In AR, a relatively clear boundary exists between the swelling rubber as the inclusion and the liquid phase as the matrix, which led to the successful back-calculation. By comparison, the absorbed bitumen is highly intersected with the undissolved rubber instead of being a shell layer of matrix around the undissolved rubber. The intertwined rubber network surrounded by bitumen molecules may provide extra reinforcing mechanisms to the swelling rubber system, so the GSCM did not fit in for this case. In other words, although the actual physical volume of undissolved rubber was obtained from the separation process, it could not represent the effective volume of inclusion in GSCM when considerable matrix is absorbed into the inclusion. The stress-strain patterns of undissolved rubber and absorbed bitumen did not follow that of inclusion and matrix assumed in GSCM, leading to the unsuccessful back-calculation. Although alternative methods are required to estimate how the mechanical property of undissolved rubber evolved during aging, these findings provide another perspective to comprehend the distribution of different phases and the internal structure of AR binder.

4.4. Rheological evolution of different phases during aging

As the internal structural change of AR binder during aging has been revealed in the volumetric and mass analysis, how the mechanical state of each phase evolves during aging deserves further analysis. The complex shear moduli of AR, liquid phase, absorbed bitumen, and swelling rubber are plotted together for comparison in Fig. 7. For clarity, only the unaged and 2PAV conditions were used to present their differences before and after aging. Since an overall good correlation existed between the master curves from DSR and micromechanical back-calculation, only the DSR results of swelling rubber were included. Meanwhile, the master curves of Pen60/70 at the two aging conditions were also presented for reference to evaluate the aging rate of AR.

At unaged condition, it can be seen that the swelling rubber performed a softening role at high-frequency region and a stiffening role at low-frequency region compared with AR and Pen60/70. As the typical modification effect of swelling rubber, it can correspondingly improve the fatigue and rutting performances of AR [18]. Meanwhile, the master curve of Pen60/70 was just between that of liquid phase and absorbed bitumen, which reflected that the absorption behavior of rubber altered the distribution of bitumen light and heavy fractions. After 2PAV aging, all master curves shifted upward due to the hardening effect of aging. The master curve of Pen60/70 occupied the highest position, which indicated that it was more vulnerable to aging than AR or any phases inside. By comparison, AR showed superior aging resistance with less changed rheological properties after aging. The different aging rates between AR and Pen60/70 have been extensively quantified in a previous study [20]. CRM improves the aging resistance of bitumen in three possible manners: 1) the rubber polymer, carbon black, and antioxidants in CRM can hinder the invasion of oxygen into the bitumen; 2) the absorption behavior of rubber can preserve the bitumen light fractions to maintain the softer mechanical property of swelling rubber, which offsets part of the bitumen hardening effect; and 3) the liquid phase can be rejuvenated when the absorbed bitumen light fractions are expelled from swelling rubber during aging [32]. By comparing the positional distribution of different curves at two aging conditions, the mechanical role changes of different phases during aging can be noticed. While the heavier fractions were thrown out into the liquid phase, the absorbed bitumen kept acting as the softest part and filling the rubber to maintain its swelling state. As a result, the liquid phase, whose mass and volume proportion rose with long-term aging, gradually became the stiffest part inside the AR system due to the increasing content of asphaltenes and dissolution of CRM. Besides, the difference between the complex share moduli of swelling rubber and AR was diminished across the whole frequency region. However, whether the mechanical property of undissolved rubber changed with aging still needs further investigation.

4.5. Chemical characterization of undissolved rubber

There are several instruments which can be used for evaluating the modulus of tire rubber, such as dynamic mechanical analysis (DMA) and nanoindentation, but these technologies are not applicable when the samples are powder-like. Therefore, this study adopted TGA and solvent-based crosslink density measurement to indirectly assess the modulus evolution of undissolved rubber during aging. In the TGA test, the thermal decomposition temperature is the fingerprint of each component. Fig. 8 shows the TGA results of undissolved rubber at unaged condition, where the TG curve represents the mass loss pattern of sample, and the DTG curve is the derivative of the mass loss curve representing the mass change rate. Points A, B, and C are three inflection points in the DTG curve dividing the components in CRM, namely additives (0–300 °C), NR (300–400 °C), SR (400–500 °C), and the reinforcing agents (>500 °C) [26,33]. Based on these rules, the concentration of each component can be calculated by the mass loss in the corresponding temperature range. Fig. 9 shows the change of different component concentrations from raw state to 2PAV aging condition, where the columns are normalized to the reinforcing agents for better comparison. The concentration of processing additive decreased rapidly from raw state to unaged condition but then remained the same afterward. It indicates that the surfactants

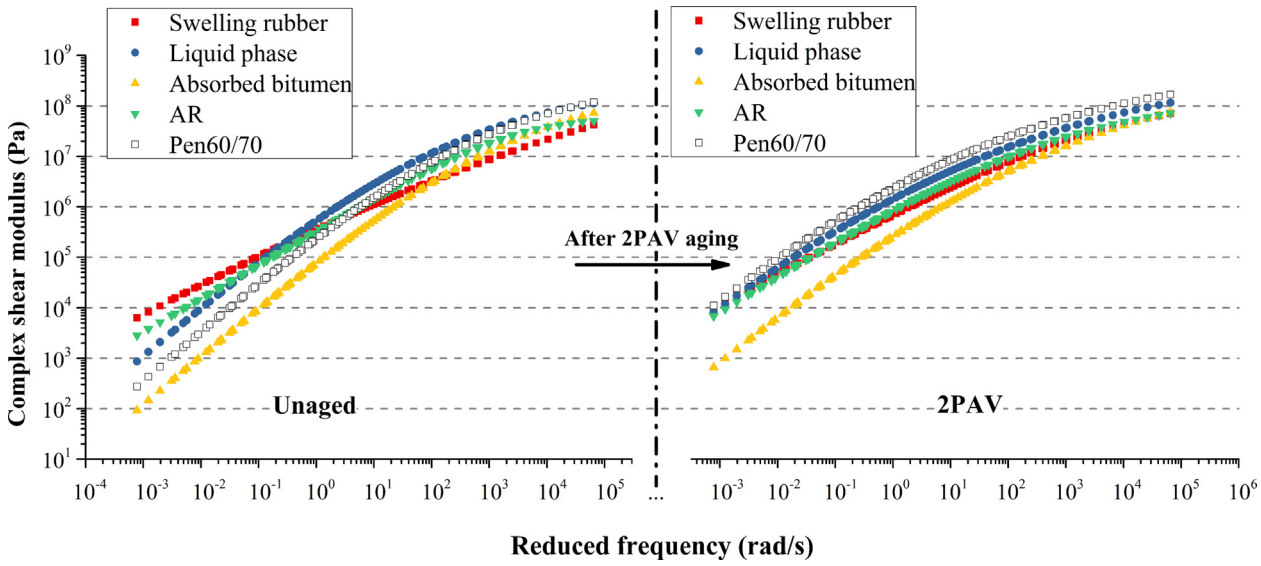

Fig. 7. Rheological characterization of different phases in AR at unaged and 2PAV aging conditions.

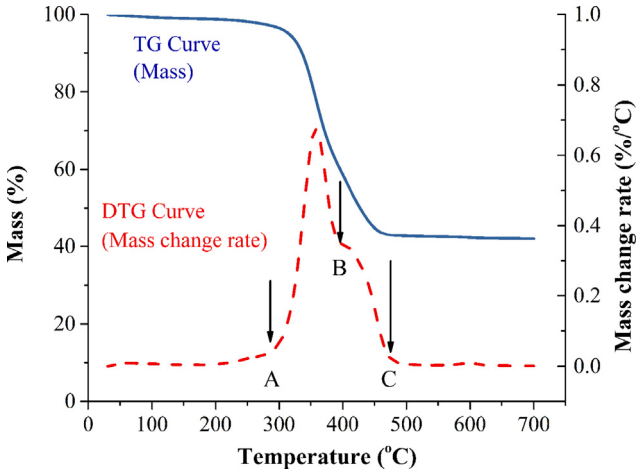

Fig. 8. TGA curves of the undissolved rubber at unaged condition.

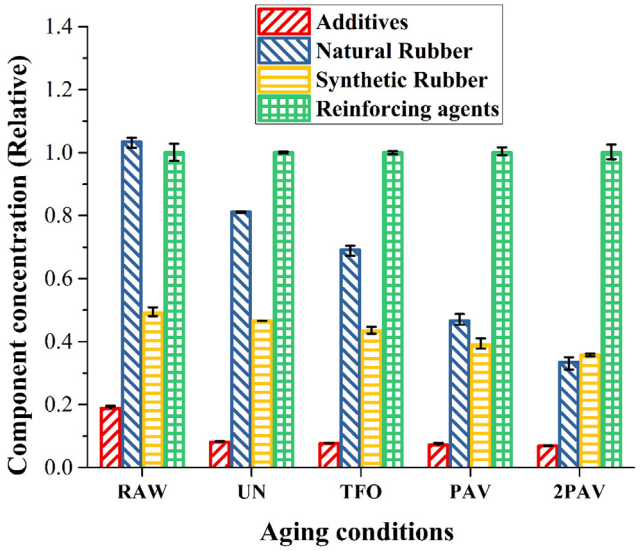

Fig. 9. Compositional variation of undissolved rubber during aging.

and oil components in CRM were totally released into bitumen during the preparation of AR. Meanwhile, an obvious decreasing trend can be observed in the concentration of NR, while that of SR just minorly decreased. NR, known as the *cis*-1,4-polyisoprene, has a simple and flexible long-chain structure, but SR as artificial rubber synthesized from petroleum by-products has more complex structures [11]. This explains why the SR is less susceptible to degradation during aging. Due to the sharp decrease in natural rubber content, the proportion of SR and reinforcing agents in undissolved rubber accordingly increased after aging. The reinforcing agents used in tire rubber include carbon black and silica fillers, which are inorganics and considered to be unsusceptible to aging in polymer science. The addition of reinforcing agents is for the purpose of improving the strength, hardness, and anti-abrasion property of tire rubber, so these agents themselves own much larger moduli than rubber polymers [34]. Furthermore, NR is reported to get softer after devulcanization and thermal-oxidative aging, but SR becomes stiffer after that [35]. Hence, it is reasonable to believe that the undissolved rubber became stiffer after aging, but the degradation of NR may soften the asphalt binder at the same time to offset the hardening effect of bitumen aging.

On the other hand, crosslink density has been suggested to be proportional to the hardness and elastic modulus of rubber [36]. Given the complex composition of tire rubber, the change of crosslink density can be attributed to the varying proportions of component with different crosslink densities. As shown in Fig. 10, the crosslink density rapidly increased from raw state to unaged because of the release of oily components into bitumen during preparation process. Afterwards, the slight decrease of crosslink density from unaged to TFO may be related to the corresponding lower liquid phase ratio of AR at TFO condition. It indicated the further swelling of rubber under the high temperature during TFO aging, where the diffused bitumen light fractions promoted the chain disentanglement of rubber polymer network. The crosslink density then started to increase from TFO to 2PAV aging condition. One major reason for this phenomenon is that the consistent decline of NR during aging reduced the proportion of low crosslink density component in undissolved rubber, while the proportion of SR owning more complex crosslinking structures became dominant [26]. Besides, the oxidation occurred during long-term aging may also complicate the microstructure inside the undissolved rubber. Therefore, combining the findings from two chemical tests,

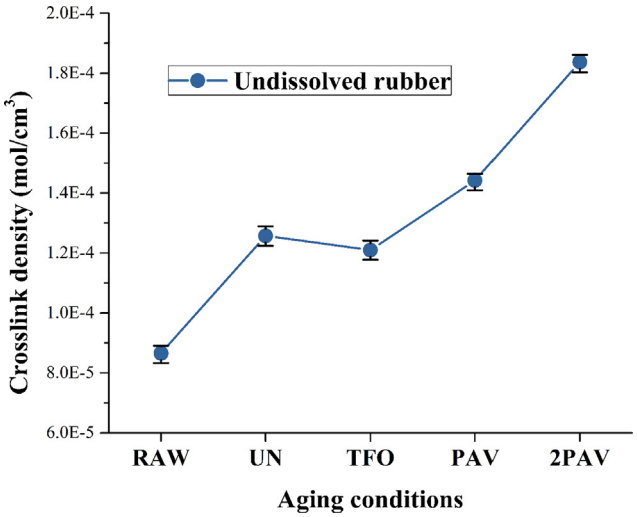

Fig. 10. Crosslink density of undissolved rubber at different aging conditions.

it could conceivably be hypothesized that the modulus of undissolved rubber in AR became larger after long-term aging.

4.6. Quantification of the mechanical role of different phases in AR during aging

Previous section has qualitatively suggested that the mechanical role of each phase in AR changed after aging. Despite this, it is still important to quantify the contribution of each phase to the overall mechanical property of AR at different frequencies, which was calculated by following Equation.

$$\Delta G_k^* = \left(1 - \frac{G_{AR}^*}{G_k^*}\right) \times 100\%, k = 1, 2, 3, 4 \quad (14)$$

where ΔG_k^* defines the mechanical contribution of each phase; k = 1, 2, 3, and 4 refer to liquid phase, absorbed bitumen, swelling rubber (DSR), and swelling rubber (GSCM), respectively; and G_{AR}^* refers to the complex shear modulus of AR. When $\Delta G_k^* > 0$, it shows a hardening effect of the certain phase, and while $\Delta G_k^* < 0$, it shows a softening effect. The results at low, intermediate, and high frequencies were summarized in Table 3, corresponding to the mechanical properties of AR at high, intermediate, and low temperatures, respectively. Different phases played different roles and cooperated with each other to compose the overall mechanical property of AR binder. The swelling rubber presented hardening effect at low frequency region and softening effect at high frequency region at unaged condition, which are the roots of the superior performance of AR binder. However, it is found that these effects of swelling rubber on the overall mechanical property of AR both weakened during aging. The softening effect of the swelling rubber at high frequency region weakened from −98.6% to −11.2% with aging due to its deteriorating swelling degree, which may result in a decline in the cracking resistance of aged AR. Meanwhile, the liquid phase offered more hardening effect than the swelling rubber at low frequency region. Although certain discrepancies existed between the results from DSR and GSCM, the overall trends were similar. Besides, the softening effect of absorbed bitumen appeared to be excessive at low-frequency region, which may imply that the mechanical contribution of absorbed bitumen is very limited at high temperature and its main function is to expand the rubber polymer network. By contrast, the absorbed bitumen presented similar or lower softening effects than swelling rubber at high-frequency region.

5. Findings and recommendations

This study investigated the structural and mechanical evolution of the multiphase system of AR binder during aging. Frequency sweep, micromechanical back-calculation, and chemical characterization were combined to assess the complex shear modulus of different phases in AR binder at different aging conditions. The following points summarize the main findings of this study:

- The multiphase structure of AR varied during aging, showing an increase in the liquid phase content and a decrease of the swelling degree of rubber due to the degradation of CRM and loss of absorbed bitumen.
- The complex moduli of swelling rubber back-calculated from micromechanical modeling correlated well with the results from experimental tests at all aging conditions, which means both ways are effective in characterizing the mechanical property of swelling rubber.
- Rheological tests and micromechanical back-calculation indicated that all bituminous phases (liquid phase, swelling rubber, and absorbed bitumen) became stiffer after aging. However, the stiffening effect of swelling rubber at low frequencies and its softening effect at high frequencies both weakened after aging while the liquid phase became the stiffest part in AR.
- TGA and crosslink density tests revealed the degradation of NR polymers and the elevated proportion of SR and reinforcing agents in undissolved rubber during aging, which symbolized its increasing modulus.

To sum up, this study reached a deeper understanding on the aging behaviors of AR and its multiphase system by using a series of innovative phase separation and characterization methods. The swelling and dissolution of rubber endowed the AR with improved performance and aging resistance, but the swelling degree of rubber inevitably deteriorated due to the bitumen aging and rubber

Table 3
Mechanical contribution of different phases to the overall system of AR.

Reduced frequency	Phase	Mechanical contribution (%)			
		Unaged	TFO	PAV	2PAV
5.63E−03	Liquid phase	−84.0	−21.5	8.5	30.9
	Swelling rubber-DSR	48.4	20.5	4.2	3.7
	Swelling rubber-GSCM	23.9	8.7	7.2	−8.0
	Absorbed bitumen	−1577.0	−1685.1	−1320.2	−615.9
5.37E+00	Liquid phase	48.5	58.7	48.6	39.3
	Swelling rubber-DSR	−17.2	−29.9	−57.2	−30.0
	Swelling rubber-GSCM	−28.9	−36.5	−50.4	−34.7
	Absorbed bitumen	−199.7	−177.4	−228.3	−169.3
4.10E+03	Liquid phase	45.6	37.5	39.7	33.5
	Swelling rubber-DSR	−98.6	−84.6	−30.7	−11.2
	Swelling rubber-GSCM	−63.3	−42.0	−27.7	−20.0
	Absorbed bitumen	−19.5	−32.5	−43.3	−31.3

degradation. Such trends are theoretically applicable for all kinds of wet-process high viscosity rubberized bitumen with a relatively high dosage of CRM > 15 wt%. Different sources of raw bitumen may affect the swelling degree of rubber at the unaged state, but it may not affect the overall aging behaviors of AR. Besides, these trends may not be suitable for the Terminal Blend (TB) type of rubberized bitumen because it emphasizes excessive dissolution of the CRM during the production stage but not the sufficient swelling condition.

The obtained findings can provide theoretical support for developing a more targeted rejuvenation method of RARP considering the structural and mechanical evolution AR during aging. Attempts can be made to combine rejuvenators and virgin AR with additional CRM to properly soften the liquid phase and supplement the amount of sufficient swelling rubber in the RARP mixture, which can recover the rheological property of RARP binder and further promote the recycling of waste tires.

CRediT authorship contribution statement

Danning Li: Conceptualization, Methodology, Formal analysis, Investigation, Data curation, Writing – original draft, Visualization. **Zhen Leng:** Resources, Writing – review & editing, Supervision, Funding acquisition, Project administration. **Haopeng Wang:** Conceptualization, Methodology. **Ruiqi Chen:** Methodology. **Frohmut Wellner:** Funding acquisition, Project administration.

Declaration of Competing Interest

The authors declare that they have no known competing financial interests or personal relationships that could have appeared to influence the work reported in this paper.

Acknowledgments

This work was supported by the RGC Germany/Hong Kong Joint Research Scheme: Aging and Recycling Mechanisms of Sustainable Asphalt Rubber Pavements (G-PolyU506/20)

Appendix A

Equations for the parameters of A, B, and C used in the GSCM are listed as follows.

$$A = 8\left(\left(\frac{G_i}{G_m}\right)-1\right)(4-5\nu_m)\eta_1\phi_i^{10/3} - 2\left(63\left(\left(\frac{G_i}{G_m}\right)-1\right)\eta_2+2\eta_1\eta_3\right)\phi_i^{\frac{7}{3}} + 252\left(\left(\frac{G_i}{G_m}\right)-1\right)\eta_2\phi_i^{5/3} - 25\left(\left(\frac{G_i}{G_m}\right)-1\right)(7-12\nu_m+8\nu_m^2)\eta_2\phi_i + 4(7 - 10\nu_m)\eta_2\eta_3 \quad (A1)$$

$$B = -4\left(\left(\frac{G_i}{G_m}\right)-1\right)(1-5\nu_m)\eta_1\phi_i^{10/3} + 4\left(63\left(\left(\frac{G_i}{G_m}\right)-1\right)\eta_2+2\eta_1\eta_3\right)\phi_i^{7/3} - 504\left(\left(\frac{G_i}{G_m}\right)-1\right)\eta_2\phi_i^{5/3} + 150\left(\left(\frac{G_i}{G_m}\right)-1\right)(3-\nu_m)\nu_m\eta_2\phi_i + 3(15\nu_m-7)\eta_2\eta_3 \quad (A2)$$

$$C = 4\left(\left(\frac{G_i}{G_m}\right)-1\right)(5\nu_m-7)\eta_1\phi_i^{10/3} - 2\left(63\left(\left(\frac{G_i}{G_m}\right)-1\right)\eta_2+2\eta_1\eta_3\right)\phi_i^{7/3} + 252\left(\left(\frac{G_i}{G_m}\right)-1\right)\eta_2\phi_i^{5/3} + 25\left(\left(\frac{G_i}{G_m}\right)-1\right)(\nu_m^2-7)\eta_2\phi_i - (5\nu_m+7)\eta_2\eta_3 \quad (A3)$$

$$\eta_1 = \left(\left(\frac{G_i}{G_m}\right)-1\right)(49-50\nu_i\nu_m) + 35\left(\left(\frac{G_i}{G_m}\right)(\nu_i-2\nu_m)+(2\nu_i-\nu_m)\right) \quad (A4)$$

$$\eta_2 = 5\nu_i\left(\left(\frac{G_i}{G_m}\right)-8\right)+7\left(\left(\frac{G_i}{G_m}\right)+4\right) \quad (A5)$$

$$\eta_3 = \left(\left(\frac{G_i}{G_m}\right)(8-10\nu_m)+(7-5\nu_m)\right) \quad (A6)$$

where G is the modulus; ν is the Poisson's ratio; and ϕ is the volumetric concentration. The subscript i and m represent inclusion and matrix, respectively.

References

[1] G.B. Way, Asphalt-rubber 45 years of progress, in: Proceedings asphalt rubber conference, Germany, 2012.
[2] X. Xu, Z. Leng, J. Lan, W. Wang, J. Yu, Y. Bai, A. Sreeram, J. Hu, Sustainable Practice in Pavement Engineering through Value-Added Collective Recycling of Waste Plastic and Waste Tyre Rubber, Engineering 7 (6) (2021) 857–867, https://doi.org/10.1016/j.eng.2020.08.020.
[3] American Society for Testing and Materials. Standard Specification for Asphalt-Rubber Binder. American Society for Testing and Materials. ASTM Standard D6114, 2009.
[4] L.G. Picado-Santos, S.D. Capitão, J.M.C. Neves, Crumb rubber asphalt mixtures: A literature review, Constr. Build. Mater. 247 (2020) 118577, https://doi.org/10.1016/j.conbuildmat.2020.118577.
[5] J.L. Feiteira Dias, L.G. Picado-Santos, S.D. Capitão, Mechanical performance of dry process fine crumb rubber asphalt mixtures placed on the Portuguese road network, Constr. Build. Mater. 73 (2014) 247–254, https://doi.org/10.1016/j.conbuildmat.2014.09.110.
[6] A. Behnood, J. Olek, Rheological properties of asphalt binders modified with styrene-butadiene-styrene (SBS), ground tire rubber (GTR), or polyphosphoric acid (PPA), Constr. Build. Mater. 151 (2017) 464–478, https://doi.org/10.1016/j.conbuildmat.2017.06.115.
[7] H. Yu, Z. Leng, Z. Zhou, K. Shih, F. Xiao, Z. Gao, Optimization of Preparation Procedure of Liquid Warm Mix Additive Modified Asphalt Rubber, J. Clean. Prod. 141 (2017) 336–345.
[8] H. Yu, Y. Chen, Q.i. Wu, L. Zhang, Z. Zhang, J. Zhang, M. Miljković, M. Oeser, Decision support for selecting optimal method of recycling waste tire rubber into wax-based warm mix asphalt based on fuzzy comprehensive evaluation, J. Clean. Prod. 265 (2020) 121781, https://doi.org/10.1016/j.jclepro.2020.121781.
[9] J. Li, Z. Chen, F. Xiao, S.N. Amirkhanian, Surface activation of scrap tire crumb rubber to improve compatibility of rubberized asphalt, Resour. Conserv. Recy. 169 (2021) 105518, https://doi.org/10.1016/j.resconrec.2021.105518.
[10] Z. Ren, Y. Zhu, Q. Wu, M. Zhu, F. Guo, H. Yu, J. Yu, Enhanced Storage Stability of Different Polymer Modified Asphalt Binders through Nano-Montmorillonite Modification, Nanomaterials 10 (2020) 641, https://doi.org/10.3390/nano10040641.
[11] H. Wang, P. Apostolidis, J. Zhu, X. Liu, A. Skarpas, S. Erkens, The role of thermodynamics and kinetics in rubber–bitumen systems: A theoretical overview, Int. J. Pavement. Eng. 22 (14) (2021) 1785–1800, https://doi.org/10.1080/10298436.2020.1724289.
[12] H. Wang, X. Liu, P. Apostolidis, M. Van de Ven, S. Erkens, A. Skarpas, Effect of Laboratory Aging on Chemistry and Rheology of Crumb Rubber Modified Bitumen, Mater. Struct. 53 (2) (2020) 26, https://doi.org/10.1617/s11527-020-1451-9.
[13] H. Wang, G. Lu, S. Feng, X. Wen, J. Yang, Characterization of bitumen modified with pyrolytic carbon black from scrap tires, Sustainability 11 (6) (2019) 1631, https://doi.org/10.3390/su11061631.
[14] C. Ouyang, S.F. Wang, Y. Zhang, Y.X. Zhang, Improving the aging resistance of styrene-butadiene-styrene tri-block copolymer modified asphalt by addition

of antioxidants, Polym. Degrad. Stab. 91 (4) (2006) 795–804, https://doi.org/10.1016/j.polymdegradstab.2005.06.009.
[15] F. Xiao, B.J. Putman, S.N. Amirkhanian, Laboratory investigation of dimensional changes of crumb rubber reacting with asphalt binder, In: Proceedings of Asphalt rubber 2006 conference, Palms Spring, California, (2006) 693–715.
[16] J.R. Medina, B.S. Underwood, Micromechanical Shear Modulus Modeling of Activated Crumb Rubber Modified Asphalt Cements, Constr. Build. Mater. 150 (2017) 56–65.
[17] H. Wang, X. Liu, P. Apostolidis, S. Erkens, A. Skarpas, Experimental investigation of rubber swelling in bitumen, Transp. Res. Rec.: J. Transp. Res. Board 2674 (2) (2020) 203–212, https://doi.org/10.1177/0361198120906423.
[18] D. Wang, D. Li, J. Yan, Z. Leng, Y. Wu, J. Yu, H. Yu, Rheological and chemical characteristic of warm asphalt rubber binders and their liquid phases, Constr. Build. Mater. 193 (2018) 547–556.
[19] H. Yu, Z. Leng, Z. Zhang, D. Li, J. Zhang, Selective absorption of swelling rubber in hot and warm asphalt binder fractions, Constr. Build. Mater. 238 (2020) 117727, https://doi.org/10.1016/j.conbuildmat.2019.117727.
[20] D. Li, Z. Leng, F. Zou, H. Yu, Effects of rubber absorption on the aging resistance of hot and warm asphalt rubber binders prepared with waste tire rubber, J. Clean. Prod. 303 (2021) 127082, https://doi.org/10.1016/j.jclepro.2021.127082.
[21] H. Zhang, K. Anupam, T. Scarpas, C. Kasbergen, S. Erkens, L. Al Khateeb, Continuum-based micromechanical models for asphalt materials: Current practices & beyond, Constr. Build. Mater. 260 (2020) 119675, https://doi.org/10.1016/j.conbuildmat.2020.119675.
[22] H. Wang, X. Liu, H. Zhang, P. Apostolidis, S. Erkens, A. Skarpas, Micromechanical modelling of complex shear modulus of crumb rubber modified bitumen, Mater. Des. 188 (2020) 108467, https://doi.org/10.1016/j.matdes.2019.108467.
[23] A. Jamrah, M.E. Kutay, S. Varma, Backcalculation of Swollen Crumb Rubber Modulus in Asphalt Rubber Binder and Its Relation to Performance, Transp. Res. Rec.: J. Transp. Res. Board 2505 (1) (2015) 99–107, https://doi.org/10.3141/2505-13.
[24] G.D. Airey, M.M. Rahman, A.C. Collop, Absorption of Bitumen into Crumb Rubber Using the Basket Drainage Method, Int. J. Pavement Eng. 4 (2) (2003) 105–119, https://doi.org/10.1080/1029843032000158879.
[25] A. Ghavibazoo, M. Abdelrahman, M. Ragab, Mechanism of Crumb Rubber Modifier Dissolution into Asphalt Matrix and Its Effect on Final Physical Properties of Crumb Rubber-Modified Binder, Transp. Res. Rec.: J. Transp. Res. Board. 2370 (1) (2013) 92–101, https://doi.org/10.3141/2370-12.
[26] H. Yao, S. Zhou, S. Wang, Structural evolution of recycled tire rubber in asphalt, J. Appl. Polym. Sci. 133 (6) (2016), https://doi.org/10.1002/app.v133.610.1002/app.42954.
[27] N. Shashidhar, A. Shenoy, On using micromechanical models to describe dynamic mechanical behavior of asphalt mastics, Mech. Mater. 34 (10) (2002) 657–669, https://doi.org/10.1016/S0167-6636(02)00166-7.
[28] H. Wang, H. Zhang, X. Liu, A. Skarpas, S. Erkens, Z. Leng, Micromechanics-based complex modulus prediction of crumb rubber modified bitumen considering interparticle interactions, Road Mater. Pavement Des. 22 (sup1) (2021) S251–S268, https://doi.org/10.1080/14680629.2021.1899965.
[29] R.M. Christensen, K.H. Lo, Solutions for effective shear properties in three phase sphere and cylinder models, J. Mech Phys. Solids 27 (4) (1979) 315–330, https://doi.org/10.1016/0022-5096(79)90032-2.
[30] L.S. Lasdon, A.D. Waren, A. Jain, M. Ratner, Design and testing of a generalized reduced gradient code for nonlinear programming, ACM T. Math. Software 4 (1) (1978) 34–50.
[31] H. Ceylan, C.W. Schwartz, S. Kim, K. Gopalakrishnan, Accuracy of Predictive Models for Dynamic Modulus of Hot-Mix Asphalt, J. Mater. Civil Eng. 21 (6) (2009) 286–293, https://doi.org/10.1061/(ASCE)0899-1561(2009)21:6(286).
[32] H. Noorvand, K. Kaloush, J. Medina, S. Underwood, Rejuvenation Mechanism of Asphalt Mixtures Modified with Crumb Rubber, Civil Eng. 2 (2021) 370–384, https://doi.org/10.3390/civileng2020020.
[33] H. Yu, Z. Leng, Z. Gao, Thermal analysis on the component interaction of asphalt binders modified with crumb rubber and warm mix additives, Constr. Build. Mater. 125 (2016) 168–174, https://doi.org/10.1016/j.conbuildmat.2016.08.032.
[34] N. Rattanasom, T. Saowapark, C. Deeprasertkul, Reinforcement of natural rubber with silica/carbon black hybrid filler, Polym. Test. 26 (3) (2007) 369–377, https://doi.org/10.1016/j.polymertesting.2006.12.003.
[35] G.R. Hamed, J. Zhao, Tensile Behavior after Oxidative Aging of Gum and Black-Filled Vulcanizates of SBR and NR, Rubber Chem. Technol. 72 (1999) 721–730, https://doi.org/10.5254/1.3538829.
[36] F. Zhao, W. Bi, S. Zhao, Influence of Crosslink Density on Mechanical Properties of Natural Rubber Vulcanizates, J. Macromol. Sci. B 50 (7) (2011) 1460–1469, https://doi.org/10.1080/00222348.2010.507453.